Spectroscopic Studies and Characterization of a Novel Electron-Transfer Chain from *Escherichia coli* Involving a Flavorubredoxin and Its Flavoprotein Reductase Partner†

Cláudio M. Gomes,‡ João B. Vicente,‡ Alain Wasserfallen,§ and Miguel Teixeira*,‡

Instituto de Tecnologia Química e Biológica, Universidade Nova de Lisboa, Rua da Quinta Grande 6, Apt 127, 2780-156, Oeiras, Portugal, and Institut für Mikrobiologie, Eidgenössische Technische Hochschule, ETH, Zürich, Switzerland

Received August 7, 2000

ABSTRACT: A novel two-component enzyme system from *Escherichia coli* involving a flavorubredoxin (FlRd) and its reductase was studied in terms of spectroscopic, redox, and biochemical properties of its constituents. FlRd contains one FMN and one rubredoxin (Rd) center per monomer. To assess the role of the Rd domain, FlRd and a truncated form lacking the Rd domain (FlRdΔRd), were characterized. FlRd contains 2.9 ± 0.5 iron atoms/subunit, whereas FlRdΔRd contains 2.1 ± 0.6 iron atoms/subunit. While for FlRd one iron atom corresponds to the Rd center, the other two irons, also present in FlRdΔRd, are most probably due to a di-iron site. Redox titrations of FlRd using EPR and visible spectroscopies allowed us to determine that the Rd site has a reduction potential of −140 ± 15 mV, whereas the FMN undergoes reduction via a red-semiquinone, at −140 ± 15 mV (Fl_{ox}/Fl_{sq}) and −180 ± 15 mV (Fl_{sq}/Fl_{red}), at pH 7.6. The Rd site has the lowest potential ever reported for a Rd center, which may be correlated with specific amino acid substitutions close to both cysteine clusters. The gene adjacent to that encoding FlRd was found to code for an FAD-containing protein, (flavo)rubredoxin reductase (FlRd-reductase), which is capable of mediating electron transfer from NADH to *Desulfovibrio gigas* Rd as well as to *E. coli* FlRd. Furthermore, electron donation was found to proceed through the Rd domain of FlRd as the Rd-truncated protein does not react with FlRd-reductase. In vitro, this pathway links NADH oxidation with dioxygen reduction. The possible function of this chain is discussed considering the presence of FlRd homologues in all known genomes of anaerobes and facultative aerobes.

Flavoproteins are catalytically extremely versatile, as their flavin coenzymes are able to perform a wide variety of enzymatic reactions comprising one-electron and two-electron transfers (*1*, *2*). The recently described recombinant flavorubredoxin (FlRd)[1] from *Escherichia coli* is an example of a novel complex flavoprotein (*3*). It consists of a unique arrangement of structural modules in which a large, partly flavodoxin-like module, is fused to a rubredoxin-like one. The flavoprotein domain of FlRd exhibits extensive sequence similarity toward other proteins, which were established as a protein superfamily originally designated by A-type flavoproteins (ATF) (*3*). This group was recently expanded in terms of additional members and characteristic sequence fingerprints (*4*, *5*). The rubredoxin domain of FlRd is found as an extension at the protein C-terminus. Rubredoxins (Rd) are small (∼6 kDa), mononuclear iron−sulfur proteins whose role remains largely elusive except in few well-documented cases such as in the *Pseudomonas*-type alkane hydroxylation system (*6*) and in the *Desulfovibrio gigas* oxygen-utilizing pathway (*7*, *8*). Quite recently, the first example of a Rd from an eukaryote was established (*9*). This novel type of Rd was found to be attached to photosystem II (*10*), which shows an unexpected wide relevance for these small electron-transfer proteins. Flavorubredoxin is a novel example of a protein having a Rd domain, after the case of rubrerythrin (*11*). Interestingly, in the genome of *Campylobacter jejuni*, the putative product of gene Cj0012c contains several non-heme iron-binding domains, including a Rd-like one (*12*).

The *Pseudomonads* and *D. gigas* pathways exploit the ability of flavoproteins to act as in vivo redox mediators, transferring electrons to other redox proteins. In both electron-transfer chains, a flavoprotein is reduced by NADH and catalyses electron transfer to a Rd, which is reoxidized by the terminal component of the pathway. Particularly interesting is the finding that a large domain of *E. coli* FlRd is identical to *D. gigas* rubredoxin:oxygen oxidoreductase (ROO) (*5*), the last element of the *D. gigas* oxygen-utilizing pathway, which was shown to interact with a Rd (*7*, *8*). Thus, the *E. coli* flavorubredoxin appears to be a fusion of a flavoprotein with its redox partner (rubredoxin). This possibility was thoroughly investigated, and we report here a novel electron-transfer chain operating in *E. coli* that mediates electron transfer between NADH and the flavoru-

† This work was supported by Grant PRAXIS XXI BIO37/96 to M.T.

* Corresponding author. Phone: 351-214469844. Fax: 351-214428766. E-mail: miguel@itqb.unl.pt.

‡ Universidade Nova de Lisboa.

§ Eidgenössische Technische Hochschule.

[1] Abbreviations: FlRd, flavorubredoxin; Rd, rubredoxin; FlRd-reductase, flavorubredoxin reductase; FlRdΔRd, rubredoxin-truncated flavorubredoxin; *orf479*, gene encoding for flavorubredoxin; *orf377*, gene encoding for flavorubredoxin reductase; *orf412* gene encoding for FlRdΔRd.

10.1021/bi001844y CCC: $19.00
Published on Web 12/01/2000

bredoxin redox cofactors as well as a characterization of the spectroscopic and redox properties of its components. This pathway also involves a flavorubredoxin reductase (FlRd-reductase) that reduces the FlRd at the expense of NADH. Interaction and kinetic studies performed using both intact and Rd domain-truncated FlRd demonstrated that the FlRd-reductase specifically reduces the Rd moiety of FlRd.

MATERIALS AND METHODS

Amplification, Cloning, and Expression. All genes were amplified from genomic DNA of *E. coli* strain XL-1 Blue (F′::Tn*10 proA*$^+$*B*$^+$ *lacI*^{q} Δ(*lacZ*)*M15*/*recA1 endA1 gyrA96* (Nal^r) *thi hsdR17* ($r_k^-m_k^+$) *supE44 relA1 lac*) with no His tag(s) attached. Gene *orf479*, which encodes for FlRd, was amplified, cloned, and expressed as described previously (*3*). The following primers were used for the amplification of *orf412* (encoding for FlRdΔRd) and *orf377* (encoding for FlRd-reductase) (restriction sites are italicized): 5′-TGAGGTT*CATATG*TCTATTG-3′ (5′ primer) and 5′-GTGGCA*AAGCTT*TATTCTTT-3′ (3′ primer, *orf412*) and 5′-GGAGGC*CATATG*AGTAACG-3′ (5′ primer) and 5′-ATCCGA*AAGCTT*AGGCAC-3′ (3′ primer, *orf377*). Amplified DNA was isolated from agarose gels, digested with restriction enzymes *Nde*I and *Hin*dIII and cloned in vector pUC28 (*13*). After verifying the amplified sequence, the genes were recloned in the expression vector pET24a (Novagen) and overexpressed overnight after induction by IPTG (20 μM final concentration), according to the manufacturer's instructions. Recombinant *E. coli* growth medium was supplemented with 10 mM Fe when the flavorubredoxin or its Rd-truncated form was expressed. The recombinant plasmids used were pME2337 (*orf479*), pME2359 (*orf412*), and pME2540 (*orf377*).

Protein Purification. Recombinant *E. coli* cells were broken using a French press at 6000 psi. The soluble extract was separated from membranes after 6 h ultracentrifugation at 42000 rpm at 4 °C and dialyzed overnight against 10 mM Tris-HCl, pH 7.6. All subsequent purification steps were performed in a HiLoad Pharmacia system. The first purification step is identical for the proteins studied. Typically, soluble extracts were applied to a Q-Sepharose (v = 30 mL) previously equilibrated with 10 mM Tris-HCl, pH 7.6. The overexpressed proteins were eluted with NaCl (FlRd at ∼450 mM and FlRd-reductase at ∼200 mM). FlRd was subsequently applied to a 70-mL gel filtration Superdex S-200 column, equilibrated and eluted with 10 mM Tris-HCl, pH 7.6, and 200 mM NaCl, 0.5 mL/min. The pink fraction was collected, dialyzed overnight, and finally applied to a Mono-Q (Pharmacia) column equilibrated with 10 mM Tris-HCl, pH 7.6, and eluted with 400 mM NaCl. FlRdΔRd was purified on 3-mL custom-packed columns eluted by stepwise salt gradients. In step 1, on Q-Sepharose (Pharmacia) equilibrated in 20 mM KP_i at pH 7, FlRdΔRd eluted with ca. 400 mM KCl. The pooled, yellowish fractions were diluted 5-fold in 10 mM Tris-HCl, pH 8.3, and applied on Fractogel EMD TMAE (Merck); the protein eluted with ca. 250 mM NaCl as pure protein as judged by SDS−PAGE gel electrophoresis. After the initial Q-Sepharose, FlRd-reductase was applied to a 5-mL prepacked Blue-Sepharose column (Pharmacia) equilibrated with 10 mM Tris-HCl, pH 7.6, and eluted with NaCl. After dialysis, the yellow fraction was run on a Mono-Q, in a procedure similarly to that described for FlRd. Pure FlRd-reductase is an FAD-containing protein. In this work, the interaction of this protein with FlRd was studied; its detailed biochemical characterization will be reported elsewhere. The purified proteins were divided in aliquots and stored at −70 °C.

Spectroscopic Methods. Room temperature UV/visible spectra were recorded on UV 1603 or Multispec 1501 diode array Shimadzu spectrophotometers. EPR spectra were obtained on a Bruker ESP 380 spectrometer equipped with an ESR 900 continuous-flow helium cryostat from Oxford Instruments.

Analytical Methods. The protein concentration was determined by the Bradford and Microbiuret methods (*14*), and iron was determined by the 2,4,6-tripyridyl-1,3,5-triazine method (*15*). Flavin HPLC analysis was done as described in ref *16*. The protein N-terminal sequence was determined using an Applied Biosystem model 470A.

Enzymatic Assays. In kinetic assays, NAD(P)H oxidation was followed at 340 nm in 10 mM Tris-HCl, pH 7.6 (ϵ^{340}_{NADH} = 6.2 mM cm^{-1}). Ferricyanide reduction (0.5 mM) was followed at 420 nm ($\epsilon^{420}_{ferricyanide}$ = 1.0 mM cm^{-1}). Oxygen consumption was measured in a YSI-Micro cell Clark-type oxygen electrode.

Redox Titrations and Analysis. Proteins were titrated anaerobically in 50 mM Tris-HCl, pH 7.6, by stepwise addition of buffered sodium dithionite (250 mM Tris-HCl at pH 8.0). The following compounds were used as redox mediators (typically 0.25−0.5 μM for visible titrations and 30−40 μM for EPR titrations): methylene blue (E'_o = 11 mV), indigo tetrasulfonate (E'_o = −30 mV), indigo trisulfonate (E'_o = −70 mV), indigo disulfate (E'_o = −182 mV), anthraquinone 2,7-disulfonate (E'_o = −182 mV), safranine (E'_o = −280 mV), neutral red (E'_o = −325 mV), benzyl viologen (E'_o = − 359 mV), and methyl viologen (E'_o = −446 mV). A silver chloride and a platinum electrode or silver/silver chloride electrodes were used, calibrated against a saturated quinhydrone solution. The reduction potentials are quoted against the standard hydrogen electrode. The experimental data were manipulated and analyzed using MATLAB (Mathworks, South Natick, MA) for Windows, which was also used for optical deconvolution and data fitting calculations. All data were adjusted to monoelectronic Nernst equations, not taking into consideration possible homotropic (electron−electron) interactions between the redox centers.

RESULTS AND DISCUSSION

Gene Locus and Proteins. Analysis of the complete *E. coli* genome (*17*) showed that the flavorubredoxin (FlRd) is encoded in a two cistron transcriptional unit, consisting of two consecutive open reading frames, *orf479* and *orf377*, forming a putative operon (Figure 1A). Upstream of *orf479* a putative promoter and a RBS sequence are found, and downstream of *orf377* a consensus terminator sequence is present. The coordinates of *orf479* and *orf377* are 2830499−2831938 and 2831935−2833068, respectively, in the sequence stored under Accession Number U00096. The FlRd is encoded by *orf479*, whereas the amino acid sequence analysis of ORF377 shows that it exhibits a significant degree of identity with Rd reductases (21−37% amino acid identity). Thus, the product of *orf377* is a potential redox partner for the flavorubredoxin, from here on named FlRd-reductase (Figure 1A,B).

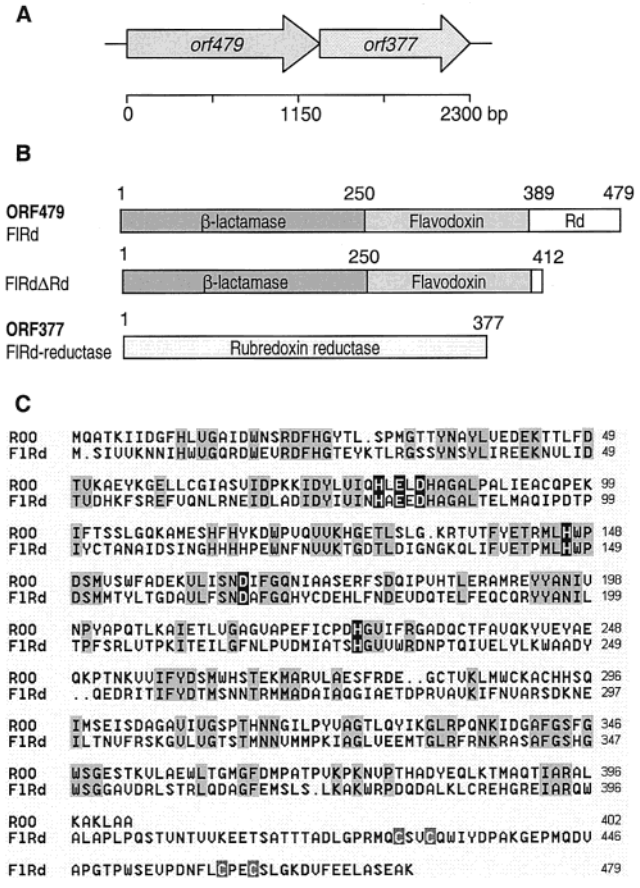

FIGURE 1: *E. coli* flavorubredoxin coding region (A), domain structure (B), and sequence alignment (C). Panel A, coding region was retrieved from NCBI GenBank. Panel B, grey shaded boxes represent distinct domains inferred from amino acid sequence analysis (*3*, *4*, this work). Panel C, pairwise amino acid sequence comparison between *E. coli* FlRd (acession U29579) and *D. gigas* ROO (acession AF218053). Black shaded boxes indicate the conserved residues that bind the binuclear iron site present in ROO; gray shaded boxes with white colored letters highlight the cysteine residues involved in binding of the Rd site in FlRd; other gray shaded boxes denote identical residues.

The *E. coli* flavorubredoxin is a multidomain protein. Sequence analysis and fold prediction using Genthreader (*18*) show that it contains a zinc β-lactamase module (residues 1−250), followed by a flavodoxin-like domain (residues 256−389), and a Rd-like extension (residues 423−479) (*3*, *5*, *8*). The Rd center binding motif (Figure 1C) indicates it is a member of the type-1 family (*31*), i.e., both cysteine motifs have the more usual CxxC spacing. An additional cofactor can be anticipated to be present in *E. coli* FlRd on the basis of recent structural data obtained for *D. gigas* ROO (*5*). The N-terminus domain of this protein was found to contain a binuclear iron site, in a β-lactamase fold, coordinated by a H-X-E-D-X_n-H-X_m-D-H motif (*5*). In fact, pairwise sequence comparisons of the first 250 amino acids of these two proteins show that they are very similar to each other (34% identity and 54% similarity) and that the bimetallic site coordinating residues are strictly conserved in *E. coli* FlRd (Figure 1C). In respect to the flavodoxin-like domain of FlRd, it is interesting to note that the similarity of this region toward the flavodoxin from *E. coli* is substantially lower (13% identity and 25% similarity) than it is in respect to other flavodoxins from other sources (typically 19−36% identity and 42−61% similarity). This

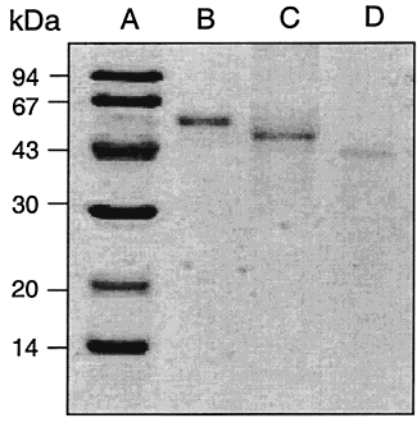

FIGURE 2: SDS−PAGE analysis of purified proteins. Lane A, molecular mass markers (Amersham/Pharmacia); lane B, FlRd (ORF479, 54.2 kDa); lane C, FlRdΔRd (ORF412, 46.8 kDa); lane C, FlRd-reductase (ORF377, 41.4 kDa).

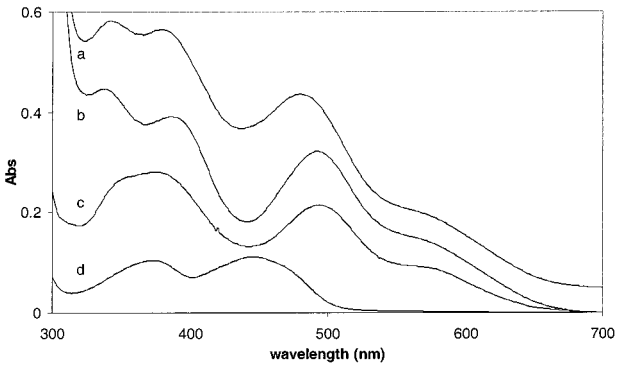

FIGURE 3: UV−visible spectra of purified proteins. Trace a, *E. coli* FlRd (≈46 μM); trace b, spectrum of the Rd domain of FlRd, obtained subtracting (1:1) spectrum of FlRd to that of FlRdΔRd; trace c, *D. gigas* Rd (≈29 μM); trace d, FlRdΔRd (≈9 μM). All proteins in 50 mM Tris-HCl, pH 7.6.

indicates that the flavodoxin domain of FlRd is not a result of a gene fusion event in the *E. coli* genome and that it arose by an independent evolutionary pathway.

To investigate the possible interaction between these *E. coli* proteins and their involvement in a putative electron-transfer system, they were purified as well as a truncated protein made from FlRd, which lacks the rubredoxin-like domain (Figure 1B). The recombinant proteins were successfully overexpressed in *E. coli* and purified to homogeneity in considerable amounts, as evaluated by clean N-terminal sequences and by 12% SDS−PAGE (Figure 2).

Flavorubredoxin Spectroscopic Characterization. Recombinant FlRd is a tetrameric protein (4 × 54 kDa) that contains one FMN/subunit (*3*). Iron quantitation of intact FlRd gives a value of 2.9 ± 0.5 iron atoms/subunit. One iron atom corresponds to the Rd center; the other two iron atoms belong most probably to the di-iron center. Consistently, the Rd truncated form of FlRd, which nevertheless comprises the residues involved in coordination of the di-iron site, has 2.1 ± 0.6 iron atoms/subunit.

The visible spectrum of *E. coli* FlRd shows features typical of flavin and Rd (Figure 3, trace a), with λ_{max} at 340, 378, and 478 nm and a broader band at 570 nm. The visible spectrum of the Rd domain truncated FlRd (FlRdΔRd) (Figure 3, trace d) lacks the typical Rd bands and solely contains pure flavinic fingerprints, with λ_{max} at 445 and 372

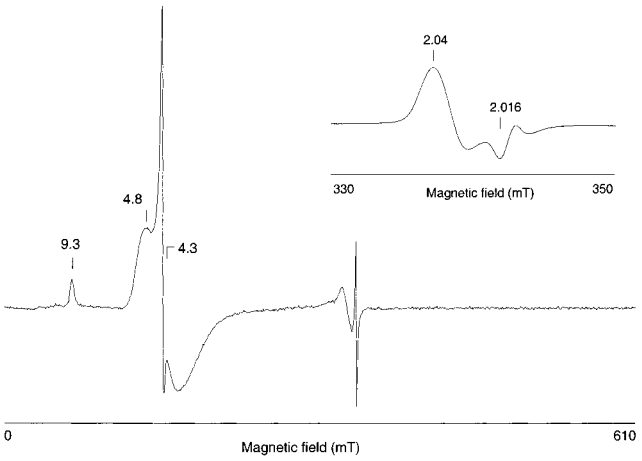

FIGURE 4: EPR spectra of *E. coli* flavorubredoxin. EPR spectrum of as prepared FlRd at 10 K. Inset, spectrum of NO-reacted, dithionite-reduced FlRd at 50 K. For both spectra: microwave power, 2.4 mW; microwave frequency, 9.44 GHz; modulation amplitude, 1 mT; protein concentration, ≈170 μM, buffer: 50 mM Tris-HCl, pH 7.6.

nm. By subtraction of these two spectra, the Rd component is obtained with λ_{max} at 575, 490, and 390 nm and a shoulder at 340 nm (Figure 3, trace b). For comparison, the spectrum of *D. gigas* Rd (*19*) is also shown (Figure 3, trace c).

The EPR spectrum of native *E. coli* FlRd is consistent with the presence of a rubredoxin-type metal center (Figure 4). Two different sets of resonances are observed, corresponding to two slightly distinct conformations of the Rd center: resonances at $g \sim 9.3$ and at $g = 4.8$ and 4.3; corresponding to a high-spin ($S = 5/2$) ferric site with $E/D \sim 0.3$ ($g_{max} = 9.6$, $|\pm 1/2>$ doublet, $g_{med} = 4.30$, $|\pm 3/2>$ doublet) and with $E/D = 0.24$ ($g_{max} = 9.35$, $|\pm 1/2>$ doublet, $g_{med} = 4.8$, $|\pm 3/2>$ doublet). At $g = 2.00$, a radical type resonance is also observed, attributable to the flavin. Upon reduction with dithionite, these features disappear as in these conditions the Rd center has an integer spin; furthermore, no other resonances develop (not shown). Native FlRdΔRd is EPR silent apart from the minor radical signal at $g = 2.00$ (not shown). No signature for a di-iron center was detected in the EPR spectrum of native (oxidized) or dithionite-reduced FlRd, as expected for an antiferromagnetically spin-coupled system, as observed for *D. gigas* ROO (*5*, *8*). No conditions could yet be found to detect the putative Fe(III)−Fe(II) species, a situation also found for *D. gigas* ROO (*5*, *8*) and for bacterioferritins (*28*, *29*). However, nitric oxide can bind to the ferrous form of iron sites. The dithionite-reduced *E. coli* FlRd reacted with NO exhibits a high-intensity EPR signal due to an $S = 1/2$ spin ground state with features at $g = 2.04$ and 2.0016 (Figure 4, inset). Similarly, the truncated FlRd displays an identical set of resonances, indicating that it also holds this metallic center (not shown). In the oxidized (as isolated) states, neither the intact nor the truncated proteins reacted with NO, suggesting that the di-iron center was in the oxidized, diferric state and thus EPR silent.

Redox Properties. The midpoint reduction potentials of the redox cofactors of FlRd were determined by redox titrations followed by visible and EPR spectroscopies. The stepwise reduction of *E. coli* FlRd in anaerobic conditions was followed by visible spectroscopy at pH 7.6 (Figure 5A). Major spectral changes occur upon reduction, with the almost

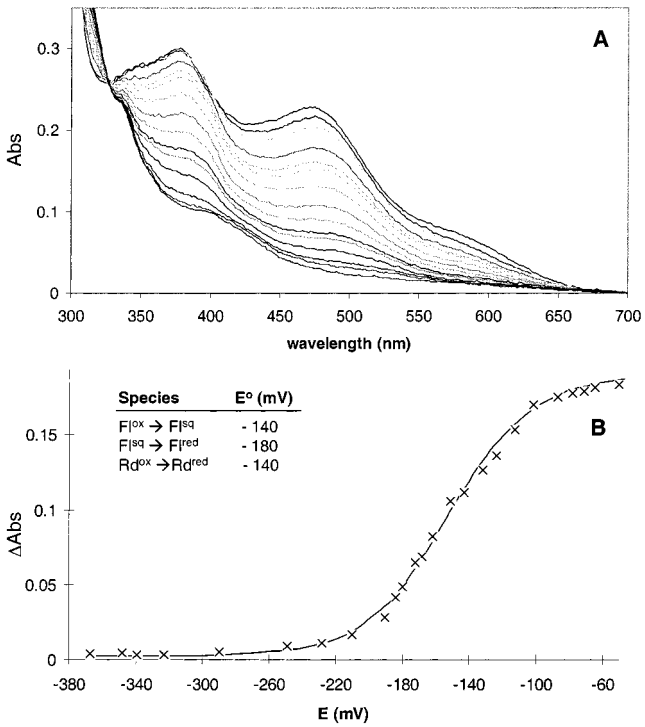

FIGURE 5: Redox titration of *E. coli* flavorubredoxin at pH 7.6. Panel A, visible spectra of FlRd (27 μM) in 50 mM Tris-HCl, pH 7.6, obtained along the redox titration. Panel B, titration curve followed at 475−425 nm. The line corresponds to a fitting to the sequential equilibrium of three one-electron-transfer steps, with $E^\circ = -140$, -140, and -180 mV, respectively. Each transition was weighted in respect to the relative contribution of each component at the working wavelength.

simultaneous bleaching of the flavin and Rd bands, which overlap below 550 nm (Figure 3). The absorbance change at 475 nm *minus* the pseudo-isosbestic point at 425 nm was plotted against the reduction potential (Figure 5B) and fitted to a Nernst curve comprising a one-electron transfer step and two consecutive one-electron transfer steps. The observed transitions were tentatively assigned to the Rd transition (Rd_{ox}/Rd_{red}, $E^\circ = -140 \pm 15$ mV) and to the flavin transitions (Fl_{ox}/Fl_{sq}, $E^\circ = -140 \pm 15$ mV and $Fl_{sq}/Fl_{red} = -180 \pm 15$ mV), respectively.

An EPR-monitored titration allowed us to assign unequivocally one of the −140 mV transitions to Rd. The amplitude of the $g = 4.3$ resonance and the height of the $g = 9.3$ signal, which decrease upon anaerobic reduction with sodium dithionite, were measured as a function of the redox potential at pH 7.6 and found to fit to a one-electron process, with $E^\circ = -140 \pm 15$ mV (Figure 6A), which completely agrees with the value obtained by following the absorbance changes at 590 nm taken from the redox titration monitored by visible spectroscopy (Figure 6A). Indeed, at this wavelength the major component in FlRd is due to the Rd center (cf. Figure 2). The midpoint reduction potential of the Rd center (−140 ± 15 mV) is significantly lower than those generally found in Rds, which range from ∼−50 to ∼30 mV, with the exception of the Rd center in rubrerythrin (∼+250 mV) (*11*) and the Rd from the eukaryotic alga *Guillardia theta* (+125 mV) (*9*, *10*). Extensive studies on the reduction potentials of Rds led to the division of Rds in two classes, distinguished by the presence of a valine or alanine after the second cysteine cluster (CPxCGX, X = A or V) (*25*). Those having

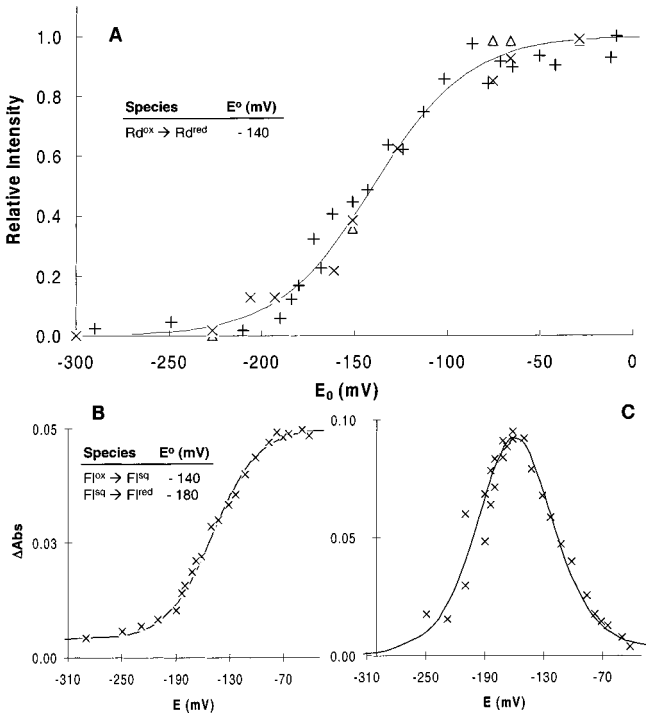

FIGURE 6: Redox titrations of FlRd constituent cofactors at pH 7.6. Panel A, titration of the FlRd Rd center followed by EPR and visible spectroscopies. The symbols (△) and (×) represent the normalized amplitudes of the $g = 4.3$ and 9.3 EPR signals, whereas (+) denotes the normalized absorbance at 590 nm. Both titrations were done in 50 mM Tris-HCl, pH 7.6. Other conditions as in Figures 4 and 5. The solid line corresponds to a Nernst process with an $E° = -140$ and $n = 1$. Panels B and C, titration of the flavin domain of FlRd. Plots were derived from data in Figure 5, except that the contribution from Rd was removed by subtracting at each working redox potential the fraction of Rd that was reduced at that potential. The spectrum of *D. gigas* Rd (Figure 3, trace c) was used in these calculations. The titrations were followed at 475−425 (B) and 380 nm (C). The lines correspond to a sequential two-step, one-electron equilibrium, with $E° = -140$ mV (Fl_{ox}/Fl_{sq}) and −180 mV (Fl_{sq}/Fl_{red}).

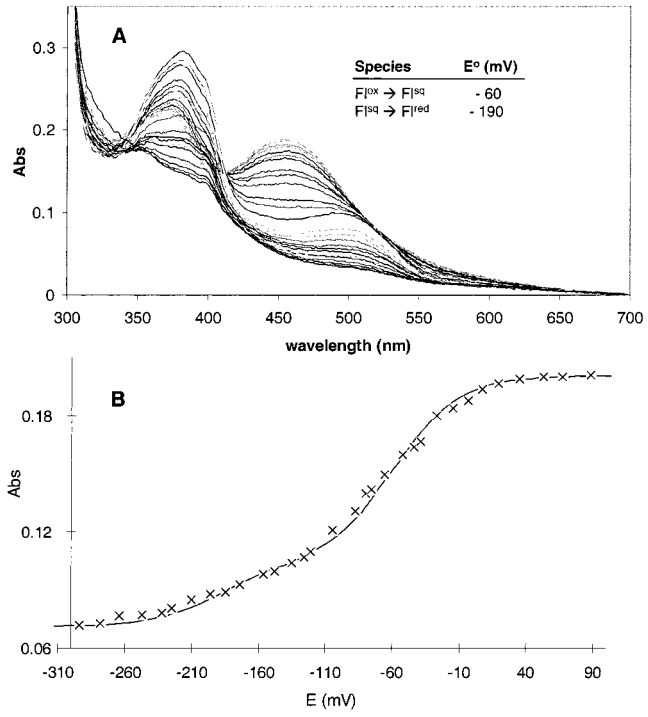

FIGURE 7: Redox titration of the rubredoxin-truncated FlRd at pH 7.6. Panel A, visible spectra of rubredoxin-truncated FlRd (15 μM) in 50 mM Tris-HCl, pH 7.6, obtained along the redox titration. Panel B, titration curve followed at 475−425 nm. The line corresponds to a sequential two-step one-electron equilibrium, with $E° = -60$ mV (Fl_{ox}/Fl_{sq}) and −190 mV (Fl_{sq}/Fl_{red}).

a valine would have a reduction potential ∼50 mV lower than those with the alanine. This change has been attributed to the influence of the dipole of the GA(V) peptide amide bond and to the strength of its hydrogen bond to the γ-S of a cysteine ligand to the iron (*20*, *21*). In *E. coli* FlRd ($E° = -140$ mV, this work) this residue is a leucine, consistent with the lower reduction potential. However, other residues have been shown to affect the reduction potential of Rds: in most of these proteins, the residues after the second cysteine of each cysteine cluster are glicines, and it has been predicted that the substitution of this residue by a bulkier amino acid, with a β-carbon, would change the hydrogen bonds to the cysteines and affect the reduction potential (*26*). In fact, mutations in *Clostridium pasteurianum* Rd have shown that the reduction potential decreases upon substituting the glycine by valine or alanine (*27*). Quite interestingly, the FlRd Rd domain has in these positions a glutamine (Gln^{432}) and a serine (Ser^{465}), substituting for glicine (Figure 1C). There are other important differences in other residues, namely, at the protein surface, that may affect also the reduction potential (*30*). In summary, the Rd site in *E. coli* FlRd shows multiple amino acid substitutions that may account for its lower reduction potential.

The remaining two consecutive one-electron transfer steps observed in the FlRd titration are attributable to FMN reduction through a semiquinone radical species. Spectral deconvolution of the FlRd titration data clearly identified the formation of a red (anionic) type flavin semiquinone during FlRd reduction (Figure 6B,C). This resulted from subtracting the basic Rd spectrum from several FlRd spectra along the titration, poising its intensity at each working redox potential, assuming a $E° = -140$ mV for the Rd site. The resulting curves exhibit characteristic features of flavin reduction via a red-type semiquinone, namely, the transient formation of absorption bands at ∼380 and ∼500 nm during reduction. The absorbance decay at 475 *minus* 425 nm follows a stepwise one-electron reduction process (Figure 6B), whereas a typical bell-shaped curve is obtained when the intensity of the band at 380 nm is plotted versus the reduction potential (Figure 6C). Fitting of the data gives midpoint reduction potentials identical to those previously estimated, $E° = -140 \pm 15$ mV (Fl_{ox}/Fl_{sq}) and $E° = -180 \pm 15$ mV (Fl_{sq}/Fl_{red}).

The Rd-truncated FlRd also undergoes reduction via a red-type semiquinone (Figure 7A). However, in this case the determined midpoint redox potentials for the two flavin transitions are different from those determined in the intact protein: -60 ± 15 mV (Fl_{ox}/Fl_{sq}) and -190 ± 15 mV (Fl_{sq}/Fl_{red}) (Figure 7B). As in this protein the Rd site is absent, it appears that in intact flavorubredoxin, either the iron−sulfur center or some of the truncated amino acid residues modulate the oxidation−reduction properties of the flavin.

The average reduction potential of the (flavo)rubredoxin reductase flavin cofactor was determined to be -170 ± 15 mV. This protein is reduced via two consecutive steps with

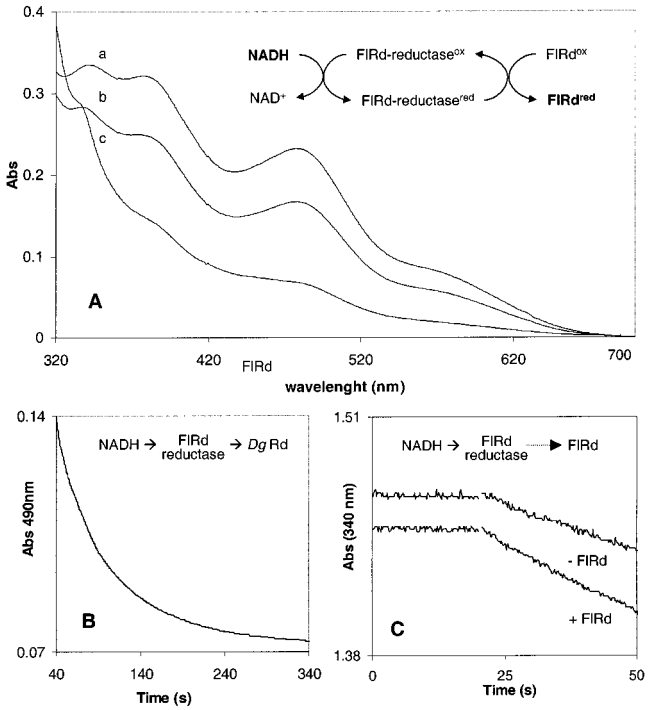

FIGURE 8: (Flavo)rubredoxin reductase is the redox partner of flavorubredoxin and electron transfer to FlRd proceeds via the Rd center. Panel A, trace a, anaerobic FlRd (28 μM) prepared in 50 mM Tris-HCl, pH 7.6, in the presence of NADH (0.3 mM). This spectrum is superimposable to that of as-prepared FlRd. Trace b, partially reduced FlRd, 1 min after addition of a catalytic amount of FlRd-reductase (2.8 μM). Trace c, reduced FlRd, 4 min after recording spectrum B. Panel B, *D. gigas* Rd (10 μM) was anaerobically reduced by FlRd-reductase (0.6 μM) and NADH (50 μM) as followed by the decay of its 490-nm band. Panel C, NADH consumption rate by FlRd-reductase (0.71 μM) in the presence of 0.24 mM NADH is increased ~1.5-fold by the presence of 14 μM FlRd (from 27 to ~40 min^{-1}). In all panels, schemes highlight the electron-transfer pathways under study.

$E° = -140 \pm 15$ mV (Fl_{ox}/Fl_{sq}) and $E° = -195 \pm 15$ mV (Fl_{sq}/Fl_{red}) (not shown).

The (Flavo)Rubredoxin Reductase Is the Redox Partner of Flavorubredoxin. The product of *orf377* has been tentatively assigned as a Rd reductase, considering its extensive amino acid sequence identity toward these proteins. Kinetically, it receives electrons from NADH at a rate of 10 min^{-1} using molecular oxygen as electron acceptor but not from NADPH. Using an oxygen electrode, the NADH-driven oxygen consumption rates measured at 25 °C in the presence and absence of externally added catalase indicated that the product of dioxygen reduction is H_2O_2 (see below and Figure 9). Ferricyanide could also be used as electron acceptor, and in this case, the K_m of the enzyme for NADH was 23 μM. The ability of FlRd-reductase to reduce a Rd center was investigated (Figure 8) using *D. gigas* Rd as electron acceptor (Figure 8B). Indeed, the product of *E. coli* ORF377 can be assigned as a true Rd reductase as the protein catalyses electron transfer from NADH to *D. gigas* Rd (20 min^{-1}) (Figure 8B) but, more importantly, also to *E. coli* FlRd at a higher rate (40 min^{-1}) (Figure 8C). These data thus provide the first indication that these two proteins interact with each other. In this context, it is worth mentioning that no Rd is encoded in the *E. coli* genome.

Another set of experiments was performed in order to clearly demonstrate the interaction between the FlRd-reductase and FlRd. Anaerobic incubation of *E. coli* FlRd with NADH does not result in any spectral changes, indicating that the protein is not reducible by this compound (Figure 8A, trace a). In agreement, FlRd shows no NAD(P)H oxidase activity. However, upon addition of a catalytic amount of FlRd-reductase, the FlRd spectra starts bleaching immediately, and full reduction is achieved within minutes, showing that the added protein is mediating electron transfer between NADH and FlRd (Figure 8A, traces b and c).

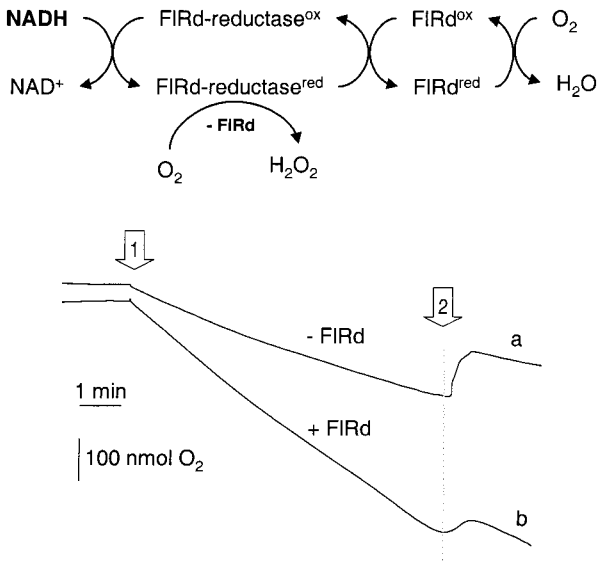

FIGURE 9: FlRd-reductase/FlRd system in vitro mediates electron transfer from NADH to oxygen and fully reduces it to water. Reaction medium contains 0.8 mM NADH in 10 mM Tris-HCl, pH 7.6, buffer. Trace a, assay in the absence of FlRd. After addition of 1.1 μM FlRd-reductase (arrow 1) oxygen uptake is at 62 min^{-1} by the FlRd-reductase and is reduced to hydrogen peroxide, as shown by the production of an amount of oxygen equivalent to ~25% of total consumed after addition of catalase (arrow 2). Trace b, assay in the presence of FlRd (23 μM) in the presence of the same amount of FlRd-reductase in trace a and, in the same conditions, results in uptake at a rate of 130 min^{-1}. In this case, oxygen reduction proceeds directly to water as addition of catalase (arrow 2) or SOD (not shown) do not result in a significant oxygen production or rate change.

The Rd center of FlRd was found to be the electron entry point in FlRd, as FlRdΔRd is not reduced by NADH/FlRd-reductase. Furthermore, *D. gigas* Rd was able to mediate electron transfer between the reductase and the truncated FlRd, thus substituting the missing cofactor. Anaerobic incubation of *D. gigas* Rd with NADH and catalytic amounts of FlRd-reductase resulted in Rd reduction, as followed by the decrease of the intensity at 490 nm (Figure 8B). However, upon anaerobic addition of FlRdΔRd, the exogenous Rd was reoxidized, showing that Rd had donated electrons to the redox cofactors present in the truncated protein (not shown).

These interaction experiments were reproduced in the oxygen electrode. Interestingly, it was observed that the NADH-driven oxygen consumption rate by FlRd-reductase increased in the presence of FlRd (from 60 to 130 min^{-1}) (Figure 9), thus suggesting that the latter could also be reducing molecular oxygen. This possibility was investigated in a set of experiments done in the presence of excess NADH, catalytic amounts of FlRd-reductase and FlRd (Figure 9, trace a). It could be observed that, in vitro, the FlRd reduces dioxygen directly to water, as the addition of catalase and/or superoxide dismutase does not alter the

Scheme 1

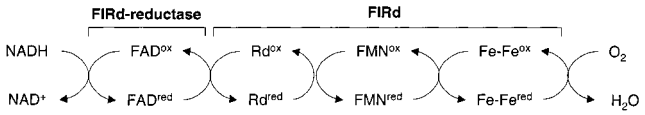

Table 1: Redox Potentials of the Cofactors Involved in the *E. coli* FlRd Electron-Transfer Chain

	$E°$ (mV)
Flavorubredoxin Reductase (FlRd-reductase)	
$FAD_{ox/sq}$ and $FAD_{sq/red}$	−140/−195
Flavorubredoxin (FlRd)	
$Rd_{ox/red}$	−140
$FMN_{ox/sq}$ and $FMN_{sq/red}$	−140/−180

oxygen consumption rate nor result in the production of oxygen (Figure 9, trace b). This activity is likely to be associated to the di-iron site, similar to what is observed in *D. gigas* ROO (*5*). In the absence of FlRd, oxygen is consumed by the FlRd-reductase, at a slower rate, and with production of hydrogen peroxide (Figure 9, trace a). In this particular case, our finding unequivocally further demonstrates that the studied proteins constitute in fact an electron-transfer chain: in the presence of FlRd, the reaction of the FlRd-reductase with oxygen occurs much slower, as electrons are more efficiently transferred to the terminal component of the pathway, the flavorubredoxin, a situation similar to that observed in *D. gigas* pathway (*7*, *8*).

CONCLUSIONS

A novel electron-transfer pathway in *E. coli*, involving a FlRd and its flavoprotein reductase partner is here described (Scheme 1). The genes encoding for these proteins cluster together in the *E. coli* genome, in a putative two cistron transcriptional unit, indicating their possible involvement in a common pathway. This was found to be the case on the basis of the redox characterization of the cofactors involved in this chain and by spectroscopic demonstration of their interactions. Indeed, the midpoint reduction potentials of these electron carriers adequately mediate electron transfer from NADH ($E°_{NADH/NAD+} = -340$ mV) to the FlRd centers (Table 1). The Rd center of FlRd, with the lowest reduction potential so far reported (-140 ± 15 mV), is a paradigmatic example of the influence of the protein backbone in adjusting the reduction potentials of a metal center.

The terminal element of this chain, FlRd, is a particularly interesting example of the modular nature of a complex flavoprotein, harboring distinct redox cofactors in a single polypeptide chain. Surprisingly, its sequence comprises a Rd domain (which is not found elsewhere in the organism's genome) that is the electron entry point in this protein. Similarly to what is observed on *D. gigas* ROO structure (*5*), it can be anticipated that in FlRd the electrons proceeding from Rd are transferred to the FMN moiety and then to the binuclear iron site, which in ROO are in van der Waals contact (*5*). Together, the flavin cofactor and the di-iron center provide the four electrons necessary to reduce dioxygen to water. The FlRd is a member of a highly conserved superfamily of proteins that are found in all known genomes of strict anaerobic archaea and bacteria, presently comprising 21 members (*3*, *4*). The pathway described here resembles the one reported for *D. gigas*, which involves a NADH: rubredoxin oxidoreductase (*22*), a Rd, and a rubredoxin: oxygen oxidoreductase (ROO) as the terminal element. In this sulfate-reducing bacterium this pathway has been shown to be involved in the response to oxygen stress, linking NAD^+ regeneration to oxygen reduction to water by ROO and thus resulting in energy conservation by substrate-level phosphorylation (*7*, *8*, *23*, *24*). Thus, it constitutes an especially safe pathway to scavenge dioxygen in an anaerobe. It was not the aim of the present work to elucidate whether a similar role is played in *E. coli* by the FlRd electron-transfer pathway. However, it may be speculated that it would play a similar function considering the need to scavenge transient oxygen species during anaerobic growth or even as a means to regenerate NAD^+ during aerobiosis. Nevertheless, a distinct function for this pathway cannot be excluded at this stage.

ACKNOWLEDGMENT

The technical skills of J. N. Carita and M. Regalla (ITQB) and S. Ragettli (ETH) are greatly acknowledged.

REFERENCES

1. Massey, V., and Hemmerich, P. (1980) *Biochem. Soc. Trans. 8*, 246−257.
2. Massey, V. (1995) *FASEB J. 9*, 473−475.
3. Wasserfallen, A., Ragettli, S., Jouanneau, Y., and Leisinger, T. (1998) *Eur. J. Biochem. 254*, 325−332.
4. Gomes, C. M., Wasserfallen, A., and Teixeira, M. (1999) *Flavins and Flavoproteins* (Ghisla, et al. Eds.) pp 219−222, Agency for Scientific Publications, Berlin.
5. Frazão, C., Silva, G., Gomes, C. M., Matias, P., Coelho, R., Sieker, L., Macedo, S., Liu, M. Y., Oliveira, S., Teixeira, M., Xavier, A. V., Rodrigues-Pousada, C., Carrondo, M. A., and LeGall, J. (2000) *Nat. Struct. Biol. 7*, 1041−1045.
6. Ruettinger, R. T., Griffith, G. R., and Coon, M. J. (1977) *Arch. Biochem. Biophys. 183*, 528−537.
7. Chen, L., Liu, M.-Y., LeGall, J., Fareleira, P., Santos, H., and Xavier, A. V. (1993) *Biochem. Biophys. Res. Commun. 193*, 100−105.
8. Gomes, C. M., Silva, G., Oliveira, S., LeGall, J., Liu, M.-Y., Xavier, A. V., Rodrigues-Pousada, C., and Teixeira, M. (1997) *J. Biol. Chem. 272*, 22502−22508.
9. Wastl, J., Sticht, H., Maier, U., Rösch, P., and Hoffmann, S. (2000) *FEBS Lett. 471*, 191−196.
10. Wastl, J., Duin, E. C., Iuzzolino, L., Dörner, W., Link, T., Hoffmann, S., Sticht, H., Dau, H., Lingelbach, K., and Maier, U. (2000) *J. Biol. Chem.* (in press).
11. Le Gall, J., Prickril, B. C., Moura, I., Xavavier, A. V., Moura, J. J., and Huynh, B. H. (1988) *Biochemistry 27*, 1636−1642.
12. Parkhill, J., et al. (2000) *Nature 403*, 665−668.
13. Benes, V., Hostomsky, Z., Arnold, L., and Paces, V. (1993) *Gene 130*, 151−152.
14. Bradford, M. M. (1976) *Anal. Biochem. 72*, 248−254.
15. Fischer, D. S., and Price, D. C. (1964) *Clin. Chem. 10*, 21−25.
16. Susín, S., Abián, J., Sánchez-Baeza, F., Peleato, M. L., Abadía, A., Gelpí, E., and Abadía, J. (1993) *J. Biol. Chem. 268*, 20958−20965.
17. Blattner, F. R., Plunkett, G., III, Bloch, C. A., Perna, N. T., et al. (1997) *Science 277*, 1453−1462.
18. Jones, D. T. (1999) *J. Mol. Biol. 287*, 797−815.
19. LeGall, J., Liu, M., Gomes, C. M., Braga, V., Pacheco, I., Xavier, A. V., and Teixeira, M. (1998) *FEBS Lett. 429*, 295−298.
20. Moura, I., Moura, J. J. G., Santos, M. H., Xavier, A. V., and LeGall, J. (1979) *FEBS Lett. 107*, 419−421.
21. Xiao, Z., Maher, M. J., Cross, M., Bond, C. S., Guss, J. M., and Wedd, G. (2000) *JBIC, J. Biol. Inorg. Chem. 5*, 75−84.

22. Eidsness, M. K., Burden, A. E., Richie, K. A., Kurtz, D. M., Scott, R. A., Smith, E. T., Ichiye, T., Beard, B., Min, T., and Kang, C. (1999) *Biochemistry 38*, 14803−14809.
23. Chen, L., Lui, M.-Y., LeGall, J., Fareleira, P., Santos, H., and Xavier, A. V. (1993) *Eur. J. Biochem. 216*, 443−448.
24. Fareleira, P., Le Gall, J., Xavier, A. V., and Santos, H. (1997) *J. Bacteriol. 179*, 3972−3980.
25. Swartz, P. D., Beck, B. W., and Ichiye, T. (1996) *Biophys. J. 71*, 2958−2969.
26. Elinor, A., Watenpaugh, K. D., and Jensen, L. H. (1975) *Proc. Natl. Acad. Sci. U.S.A. 72*, 4854−4858.
27. Maher, M. J., Xiao, Z., Wilce, M. C. J., Guss, J. M., and Wedd, A. G. (1999) *Acta Crystallogr. D55*, 962−968.
28. Romão, C. M., Regalla, M., Xavier, A. V., Teixeira, M., Liu, M.-Y., and LeGall, J. (2000) *Biochemistry 39*, 6841−6849.
29. Le Brun, N. E., Wilson, M. T., Andrews, S. C., Guest, J. R., Harrison, P. M., Thomson, A. J., and Moore, G. R. (1993) *FEBS Lett. 333*, 197−202.
30. Zeng, Q., Smith, E. T., Kurtz, D. M., and Scott, R. A. (1996) *Inorg. Chim. Acta 242*, 245−251.
31. LeGall, J., Liu, M. Y., Gomes, C. M., Braga, V., Pacheco, I., Regalla, M., Xavier, A. V., and Teixeira, M. (1998) *FEBS Lett. 429*, 295−298.

BI001844Y